SLAC-PUB-12314
January 2007

Automatic quenching of high energy γ-ray sources by synchrotron photons

Łukasz Stawarz[1,2] and John Kirk[3]

[1] *Kavli Institute for Particle Astrophysics and Cosmology, Stanford University, Stanford, CA 94305*

[3] *Max-Planck-Institut für Kernphysik, Saupfercheckweg 1, 69117 Heidelberg, Germany*

ABSTRACT

Here we investigate evolution of a magnetized system, in which continuously produced high energy emission undergoes annihilation on a soft photon field, such that the synchrotron radiation of the created electron-positron pairs increases number density of the soft photons. This situation is important in high energy astrophysics, because, for an extremely wide range of magnetic field strengths (nano to mega Gauss), it involves γ-ray photons with energies between 0.3 GeV and 30 TeV. We derive and analyze the conditions for which the system is unstable to runaway production of soft photons and ultrareltivistic electrons, and for which it can reach a steady state with an optical depth to photon-photon annihilation larger than unity, as well those for which efficient pair loading of the emitting volume takes place. We also discuss the application of our analysis to a realistic situation involving astrophysical sources of a broad-band γ-ray emission and briefly consider the particular case of sources close to active supermassive black holes.

Subject headings: radiation mechanisms: non-thermal — gamma-rays: theory — galaxies: active

1. Introduction

Astrophysical sources of high energy X-ray and γ-ray radiation are often compact enough to make the effects of photon-photon annihilation and subsequent emission of secondary particles significant (Jelley 1966; Bonometto & Rees 1971; Herterich 1974; Guilbert et al.

[2] Also at SLAC, MenloPark CA 94025; and Astronomical Observatory of the Jagiellonian University, ul. Orla 171, 30-244 Kraków, Poland. E-mail: `stawarz@slac.stanford.edu`

Submitted to ApJLetters

Work supported in part by the US Department of Energy contract DE-AC02-76SF00515

1983; Kazanas 1984), leading to the development of electromagnetic cascades. In many situations, it is appropriate to assume that the cascades are linear, in the sense that the density of target photons can be taken to be fixed. This situation is particularly convenient for a Monte-Carlo computation of the emergent spectrum (e.g., Akharonian et al. 1985; Protheroe 1986). Nonlinearity arises when photons produced by the cascading electron-positron pairs are themselves targets in the photon-photon pair-production process. This situation has been considered mostly in connection with compact X-ray sources (Svensson 1987; Zdziarski 1988), where photons that are inverse-Compton scattered by the nonthermal pairs form the target population.

Using simplified kinetic equations, Zdziarski & Lightman (1985) studied steady state radiative spectra of non-thermal electrons in active galactic nuclei subjected to inverse-Compton and synchrotron energy losses, taking photon-photon annihilation and the resulting production of a first generation of secondary electron-positron pairs within the emission region into account self-consistently. A similar discussion was also presented by Fabian et al. (1986) and Lightman & Zdziarski (1987), who investigated the spectra of such sources for a wide range of parameters and included the effects of thermal pairs. Facilitated by the dramatic improvement in computing resources, algorithms for the computation of time-dependent solutions of the kinetic equations describing these processes have developed by several groups (e.g., Coppi 1992; Mastichiadis & Kirk 1995; Stern et al. 1995) and are routinely used in source modelling (Konopelko et al. 1999; Krawczynski et al. 2002)

Recently, however, attention has focused on the intrinsically nonlinear effects. Kirk & Mastichiadis (1992) studied the conditions under which ultrarelativistic protons could initiate runaway pair-production. In the application to active galactic nuclei, the required parameter range is extreme, but gamma-ray bursts provide a more promising environment (Kazanas & Mastichiadis 1999; Kazanas et al. 2002; Mastichiadis & Kazanas 2006). A strong feedback mechanism has also been identified which may mediate relativistic shocks (Stern 2003), or, in the case of relativistic jets, act as a breeding mechanism for high energy γ-rays (Stern & Poutanen 2006).

In this *Letter* we analyse the conditions under which a magnetized system, with an embedded source of high energy photons of energy $\varepsilon \equiv \epsilon\, m_{\rm e} c^2$ can initiate and sustain pair production autonomously. The nonlinear process that makes this possible is annihilation on soft photons with energies $\varepsilon_0 \equiv \epsilon_0\, m_{\rm e} c^2$, that are produced as the synchrotron emission of the created electron-positron pairs. We assume an isotropic distribution of the high energy and soft photon fields in the source rest frame, as well as $\epsilon \gg 1$, which implies $\epsilon = 2/\epsilon_0 \gg \epsilon_0$ and $\gamma = \epsilon/2 \gg 1$. The process operates when the magnetic field B is such that $\epsilon_0 = (4/3)\,(B/B_{\rm cr})\,\gamma^2$, where $B_{\rm cr} = 2\pi\, m_{\rm e}^2 c^3/h\, e \approx 4.4 \times 10^{13}\,{\rm G}$. Therefore, we

investigate the behavior of systems where

$$B \;=\; 6\, B_{\rm cr}\, \epsilon^{-3} \tag{1}$$

or $B = 265\,(\epsilon/10^6)^{-3}\,\mu$G $= 35\,(\varepsilon/{\rm TeV})^{-3}\,\mu$G. Such systems are important in high energy astrophysics, because for an extremely wide range of magnetic field strengths ($B = 10^{-9}\,{\rm G}-10^6\,{\rm G}$) Eq. (1) is satisfied for photon energies between $\varepsilon \approx 0.3\,{\rm GeV}$ and $30\,{\rm TeV}$, that are accessible to space or ground based γ-ray observatories.

2. Equations

We restrict our analysis to the high energy and soft photon populations with characteristic energies ϵ and ϵ_0, respectively, that interact with ultrarelativistic electrons and positrons (henceforth simply called "electrons") of characteristic Lorentz factor γ. In the systems of interest, the radiative cooling time scale of these electrons is much shorter than the light-crossing time of the emitting volume, and we assume that no other process such as acceleration, or interaction with background particles or waves is able to compete with the cooling. Although our formulation does not enable us to extract detailed spectral information, we discuss the implications for the case of a broad-band spectrum of high energy photons.

We denote the total number of high energy photons, soft photons, and the created electrons in our source by N, N_0 and $N_{\rm e}$, and work with the effective logarithmic number densities defined by $\mathcal{N}(\epsilon) = N/\epsilon\mathcal{V}$, $\mathcal{N}_0(\epsilon_0) = N_0/\epsilon_0\mathcal{V}$, $\mathcal{N}_{\rm e}(\gamma) = N_{\rm e}/\gamma\mathcal{V}$. The appropriate set of kinetic equations can be then written as

$$\frac{{\rm d}\mathcal{N}(\epsilon)}{{\rm d}t} \;=\; \dot{\mathcal{N}}^{\gamma\gamma}(\epsilon) + \dot{\mathcal{N}}^{\rm esc}(\epsilon) + \mathcal{Q}(\epsilon) \quad ,$$

$$\frac{{\rm d}\mathcal{N}_0(\epsilon_0)}{{\rm d}t} \;=\; \dot{\mathcal{N}}_0^{\rm esc}(\epsilon_0) + \dot{\mathcal{N}}_0^{\rm syn}(\epsilon_0) \quad ,$$

and

$$\frac{{\rm d}\mathcal{N}_{\rm e}(\gamma)}{{\rm d}t} \;=\; \dot{\mathcal{N}}_{\rm e}^{\gamma\gamma}(\gamma) + \dot{\mathcal{N}}_{\rm e}^{\rm syn}(\gamma) + \dot{\mathcal{N}}_{\rm e}^{\rm ic}(\gamma) \tag{2}$$

(see Zdziarski & Lightman 1985; Fabian et al. 1986). The terms on the right-hand sides of the above equations are as follows: (i) The high energy photons are assumed to be continuously injected into the emission volume $\mathcal{V} = \pi R^3$ at the rate $\mathcal{Q}(\epsilon) = L_{\rm inj}/(\epsilon^2\, m_{\rm e} c^2\, \mathcal{V})$, where $L_{\rm inj}$ is the high energy luminosity intrinsic to the source. They undergo photon-photon annihilation at the rate $\dot{\mathcal{N}}^{\gamma\gamma}(\epsilon) = -c\,\alpha_{\gamma\gamma}\,\mathcal{N}(\epsilon)$, with $\alpha_{\gamma\gamma} = (2/3)\,\sigma_{\rm T}\,\epsilon^{-1}\,\mathcal{N}_0(\epsilon_0)$, as follows from the approximate expression for the photon-photon annihilation cross section,

$\sigma_{\gamma\gamma}(\epsilon,\epsilon_0) = (1/3)\,\sigma_{\rm T}\,\epsilon_0\,\delta\,[\epsilon_0 - (2/\epsilon)]$ given by Zdziarski & Lightman (1985). In addition, they escape from the system, assumed to be roughly spherical with radius R, at the rate $\dot{\mathcal{N}}^{\rm esc}(\epsilon) = -\mathcal{N}(\epsilon)/t_{\rm esc}$ with $t_{\rm esc} = R/c$ (this expression can be regarded as the definition of the effective radius R). (ii) The soft photons are produced by the synchrotron emission of the created electron-positron pairs at the rate $\epsilon_0\dot{\mathcal{N}}_0^{\rm syn}(\epsilon_0) = 4\pi\, j_{\epsilon_0}/(m_{\rm e}c^2)$, where the synchrotron emissivity can be evaluated as $\epsilon_0 j_{\epsilon_0} = \gamma\,\mathcal{N}_{\rm e}(\gamma)\,|\dot{\gamma}|_{\rm syn}\,m_{\rm e}c^2/(8\pi)$ with the synchrotron energy losses term $|\dot{\gamma}|_{\rm syn} = (4\,c\sigma_{\rm T}/3\,m_{\rm e}c^2)\,U_{\rm B}\,\gamma^2$, and the magnetic field energy density $U_{\rm B} = B^2/8\pi$. As in the case of hard photons, soft photons escape from the system at the rate given by $\dot{\mathcal{N}}_0^{\rm esc}(\epsilon_0) = -\mathcal{N}_0(\epsilon_0)/t_{\rm esc}$ with $t_{\rm esc} = R/c$. (iii) Electron-positron pairs are injected via the photon-photon annihilation process so that $\dot{\mathcal{N}}_{\rm e}^{\gamma\gamma}(\gamma) = -4\dot{\mathcal{N}}^{\gamma\gamma}(\epsilon)$, since $\gamma \approx \epsilon/2$ (see Coppi & Blandford 1990). They also undergo radiative cooling, modeled here as catastrophic escape from the analyzed energy range. For synchrotron radiation the appropriate rate is then $\dot{\mathcal{N}}_{\rm e}^{\rm syn}(\gamma) = -\mathcal{N}_{\rm e}(\gamma)/t_{\rm syn}$ where $t_{\rm syn} = \gamma/|\dot{\gamma}|_{\rm syn}$. For inverse-Compton cooling the rate is $\dot{\mathcal{N}}_{\rm e}^{\rm ic}(\gamma) = -\mathcal{N}_{\rm e}(\gamma)/t_{\rm ic}$ with $t_{\rm ic} = \gamma/|\dot{\gamma}|_{\rm ic}$. The inverse-Compton loss term can be written $|\dot{\gamma}|_{\rm ic} = (4\,c\sigma_{\rm T}/3\,m_{\rm e}c^2)\,U_0\,\gamma^2\,\eta^{-1}$, where the energy density of the soft photons is $U_0 = \epsilon_0^2\,m_{\rm e}c^2\,\mathcal{N}_0(\epsilon_0)$, and the additional factor $\eta \approx 5^{1.5}$ takes adequate account of Klein-Nishina effects, since $\gamma\,\epsilon_0 = 1$ and we do not consider the detailed spectral shape (see Moderski et al. 2005). The direct influence of inverse-Compton scattering and annihilation on the soft photon field is negligibly small provided $\gamma \gg 1$ and $\epsilon \gg 1$.

Our system thus has three free parameters, ϵ (or B), R and $L_{\rm inj}$, and three variables, $\mathcal{N}(\epsilon)$, $\mathcal{N}_0(\epsilon_0)$ and $\mathcal{N}_{\rm e}(\gamma)$. It is convenient to express the parameters in terms of dimensionless quantities: the high-energy injection compactness and the magnetic compactness,

$$\ell_{\rm inj} \equiv \frac{\epsilon\,L_{\rm inj}\,\sigma_{\rm T}}{4\pi\,m_{\rm e}c^3\,R} \quad \text{and} \quad \ell_{\rm B} \equiv \frac{\epsilon\,U_{\rm B}\,R\,\sigma_{\rm T}}{m_{\rm e}c^2} \quad . \tag{3}$$

Note that these quantities contain a factor ϵ not present in the conventional definitions (Guilbert et al. 1983). Instead of the soft photon number density we use the equivalently the optical depth for photon-photon annihilation

$$n_0 \equiv \tau_{\gamma\gamma} = \frac{2\,\sigma_{\rm T}\,R}{3\,\epsilon}\,\mathcal{N}_0(\epsilon_0) \quad , \tag{4}$$

and instead of the hard photon number density, we use the ratio of the hard photon energy density to the energy density of soft photons needed to give $\tau_{\gamma\gamma} = 1$:

$$n \equiv \frac{U}{U_0|_{\tau_{\gamma\gamma}=1}} = \frac{\epsilon^3\,\sigma_{\rm T}\,R}{6}\,\mathcal{N}(\epsilon) \quad , \tag{5}$$

Similarly, for the electron density we use the ratio of the energy density to that of soft photons required for $\tau_{\gamma\gamma} = 1$,

$$n_{\rm e} \equiv \frac{U_{\rm e}}{U_0|_{\tau_{\gamma\gamma}=1}} = \frac{\epsilon^3\,\sigma_{\rm T}\,R}{24}\,\mathcal{N}_{\rm e}(\gamma) \quad . \tag{6}$$

and measure time in units of the light crossing time $\tau \equiv ct/R$. This leads to the autonomous dynamical system:

$$\begin{aligned} \frac{\mathrm{d}\,n}{\mathrm{d}\tau} &= -n\,n_0 - n + \frac{2}{3}\,\ell_{\rm inj} \\ \frac{\mathrm{d}\,n_0}{\mathrm{d}\tau} &= -n_0 + \frac{1}{3}\,\ell_{\rm B}\,n_{\rm e} \\ \frac{\mathrm{d}\,n_{\rm e}}{\mathrm{d}\tau} &= n\,n_0 - \frac{2}{3}\,\ell_{\rm B}\,n_{\rm e} - \frac{4}{\eta}\,n_{\rm e}\,n_0 \quad . \end{aligned} \tag{7}$$

Note, that the coefficients in this system do not depend explicitly on ϵ.

3. Stationary solutions and their stability

For all physical values of the parameters $\ell_{\rm inj} > 0$ and $\ell_{\rm B} > 0$ there exists a trivial stationary solution of the system (7): $n = 2\ell_{\rm inj}/3$, $n_0 = 0$, $n_{\rm e} = 0$, corresponding to free propagation of the hard photons through a medium in which pairs and soft photons are completely absent. The eigenvalues of the Jacobian matrix evaluated for this solution are all real. For $\ell_{\rm inj} < 3$ they are all negative, so that the solution is stable in this region. This means that the nonlinearity is not sufficient for the system to initiate and sustain a population of pairs if $\ell_{\rm inj} < 3$. Furthermore, in this region, no other physically realistic ($n_0 > 0$, $n_{\rm e} > 0$) stationary solution exists.

For $\ell_{\rm inj} > 3$, at least one of the eigenvalues has a positive real part, so that the solution in which pairs are absent is unstable. However, in this region a second stationary solution emerges, with

$$\begin{aligned} n &= \frac{2\ell_{\rm inj}}{3\,(1+n_0)} \\ n_{\rm e} &= \frac{3n_0}{\ell_{\rm B}} \\ n_0 &= \frac{1}{12}\left[-6 - \eta\ell_{\rm B} + \sqrt{(\eta\ell_{\rm B}-6)^2 + 8\eta\ell_{\rm B}\ell_{\rm inj}}\right] . \end{aligned} \tag{8}$$

Using the Routh-Hurwitz conditions (Gradshteyn & Ryzhik 1980, 17.715), one can show that the real parts of the eigenvalues of the Jacobian matrix corresponding to this physical solution are negative, so that the solution is stable.

Figure 1 illustrates the properties of the stable solutions of this system on the $\ell_{\rm B}$–$\ell_{\rm inj}$ plane. The horizontal dotted line $\ell_{\rm inj} = 3$ bounds from above the region (shaded dark gray) in which the stable solution contains neither pairs nor soft photons, so that $\tau_{\gamma\gamma} = 0$. The

solid line, on which $\ell_{\rm inj} = 6+36/(\eta\,\ell_{\rm B})$, is the locus of points at which the stable solution has unit optical depth to absorption of high energy photons: $n_0 = \tau_{\gamma\gamma} = 1$. Strictly speaking, our treatment of the escape probability of hard photons is valid only in the optically thin case $\tau_{\gamma\gamma} < 1$, which is shaded light gray. However, for $\ell_{\rm inj} > 6 + 36/(\eta\,\ell_{\rm B})$, (white area) we expect on physical grounds that the system tends spontaneously to an optically thick state with almost total absorption of the hard photons.

Stable solutions which have equal energy densities of soft and hard photons ($n = n_0$) occur formally when $\ell_{\rm inj} = 3\eta\ell_{\rm B}(3\eta\ell_{\rm B} - 12)/(\eta\ell_{\rm B} - 12)^2$, shown as a thick dashed line. This line lies entirely within the optically thick region. Thus, our system is valid only for solutions in which the energy density of soft photons is small compared to that in hard photons.

Finally, stable solutions in which the electron and magnetic field energy densities are equal occur when $U_{\rm e}/U_{\rm B} \equiv 6\,n_{\rm e}/\ell_{\rm B} = 1$, shown as a thick dotted line. Solutions which are particle dominated lie above this line in the hatched region of Fig. 1. It is interesting to note that when the optical depth for photon-photon annihilation is less than unity, $\tau_{\gamma\gamma} < 1$, stable solutions can be found that are pair dominated, in the sense that the electron energy density exceeds that in the magnetic field. These solutions occur in the intersection of the hatched and light gray areas of Fig. 1. They imply efficient pair-loading of the system and are particularly relevant for $\ell_{\rm B} \ll 1$, where they occur for all relevant injection compactnesses $\ell_{\rm inj} > 3$.

4. Applications

The electrons created in the photon-photon annihilation process cool due to synchrotron and inverse-Compton energy losses. In the analysis presented so far, where a monoenergetic high energy photon field was considered, with fixed photon energy $\epsilon = \epsilon^\star$, these losses were modeled as a escape of particles from the chosen energy range. In a more precise treatment, the electrons do not escape catastrophically, but cool to form a distribution given by

$$\mathcal{N}_{\rm e}(\gamma) \;=\; \frac{1}{|\dot\gamma|_{\rm cool}} \int_\gamma^\infty {\rm d}\gamma' \mathcal{Q}_{\rm e}(\gamma') \tag{9}$$

Here $\mathcal{Q}_{\rm e}(\gamma)$ denotes injection rate of high-energy electrons via photon-photon annihilation, and $|\dot\gamma|_{\rm cool} = |\dot\gamma|_{\rm syn} + |\dot\gamma|_{\rm ic}$ is the total radiative cooling rate of these electrons. In the systems considered here, inverse Compton cooling occurs in the transition region between Thomson and Klein-Nishina scattering. Consequently, we can approximately write $\gamma_{\rm cool} \propto \gamma^2$. Thus, below the injection energy $\gamma^\star = \epsilon^\star/2$ the steady state spectrum of the cooled electrons is $N_{\rm e}(\gamma < \gamma^\star) \propto \gamma^{-2}$, leading to a synchrotron spectrum at photon energies $\epsilon_0 < \epsilon_0^\star =$

$2/\epsilon^\star$ corresponding to an emissivity $j_{\epsilon_0<\epsilon_0^\star} \propto {\epsilon_0}^{-1/2}$. In turn these photons absorb high-energy radiation with photon energies $\epsilon > \epsilon^\star$. Since the optical depth for the photon-photon annihilation is $\tau_{\gamma\gamma} \propto \epsilon_0 \mathcal{N}_0(\epsilon_0) \propto j_{\epsilon_0}$, the condition for $\tau_{\gamma\gamma} > 1$ at $\epsilon = \epsilon^\star$ ensures automatically $\tau_{\gamma\gamma} > 1$ for any $\epsilon > \epsilon^\star$. In other words, if the parameters of the considered system are such that it becomes optically thick for the high energy photons with $\epsilon^\star$, then all the emission at higher photon energies $\epsilon > \epsilon^\star$ will also be absorbed. For the intrinsic luminosity $L_{\rm inj}$ corresponding to the photon energies $\epsilon^\star$, the appropriate condition for $\tau_{\gamma\gamma}(\epsilon > \epsilon^\star) > 1$ can be therefore expressed as $L_{\rm inj} \geq L_{\rm crit}$ with

$$\left(\frac{L_{\rm crit}}{10^{45}{\rm erg/s}}\right) \;=\; 10^{-11}\left(\frac{\varepsilon^\star}{\rm GeV}\right)^4 + 4.4\left(\frac{R}{\rm pc}\right)\left(\frac{\varepsilon^\star}{\rm GeV}\right)^{-1} \tag{10}$$

(see Eq. 8), where $\varepsilon^\star$ is directly related to the magnetic field (see Eq. 1).

The immediate vicinities of supermassive black holes (SMBHs) in active galactic nuclei constitute an interesting case for the process discussed here. It has been suggested that these objects accelerate protons to ultra-high energies of $\geq 10^{20}\,$eV (Boldt & Ghosh 1999; Boldt & Loewenstein 2000), generating very high energy γ-ray emission (Levinson 2000). Magnetic field intensities in such systems are expected to be high: a common approach is to assume equipartition between pressures of the magnetic field and of radiation produced by the accreting matter. This gives

$$B = \left(\frac{R}{r_{\rm g}}\right)^{-1}\left(\frac{L_{\rm acc}}{L_{\rm Edd}}\right)^{1/2}\left(\frac{L_{\rm Edd}}{r_{\rm g}^2 c}\right)^{1/2}, \tag{11}$$

where $r_{\rm g} = G\,\mathcal{M}/c^2 \approx 1.5\times 10^{13}\,\mathcal{M}_8\,{\rm cm}$ is the Schwarzchild radius of the black hole with mass $\mathcal{M} \equiv \mathcal{M}_8\,10^8\,M_\odot$, $L_{\rm acc}$ is the accretion luminosity produced within radius R, and $L_{\rm Edd} = 4\pi\,G\,\mathcal{M}\,m_{\rm p}\,c/\sigma_{\rm T} \approx 1.3\times 10^{46}\,\mathcal{M}_8\,{\rm erg\,s^{-1}}$ is the corresponding Eddington luminosity. SMBHs typically have masses $\mathcal{M}_8 \sim (10^{-2}-10^2)$ and luminosities $L_{\rm acc}/L_{\rm Edd} \sim (10^{-7}-1)$, so that the appropriate range of the magnetic field within the nuclear regions of $R \sim {\rm few}\times r_{\rm g} \sim (10^{-7}-10^{-3})\,{\rm pc}$ is $B \sim (10^{-1}-10^4)\,{\rm G}$. For such parameters, $L_{\rm crit}$ values are shown in Figure 2 (see the left y-axis) as dark gray area in between of the thick solid and dashed lines corresponding to $R = 10^{-3}\,{\rm pc}$ and $R = 10^{-7}\,{\rm pc}$, respectively.

Despite the huge parameter range considered, one can conclude that in the case of active nuclei hosting the most massive black holes and accreting at the highest rates (e.g., quasars with $\mathcal{M}_8 > 1$ and $L_{\rm acc}/L_{\rm Edd} > 10^{-3}$), no high energy γ-ray emission at photon energies $\varepsilon \geq \varepsilon^\star \sim (1-10)\,{\rm GeV}$ emerging from the closest vicinities of SMBHs should be expected with $\varepsilon^\star L_{\varepsilon^\star} \geq (10^{41}-10^{42})\,{\rm erg\,s^{-1}}$. For AGNs with similarly massive black holes but accreting at lower rates ($L_{\rm acc}/L_{\rm Edd} < 10^{-3}$; e.g., FR I radio galaxies), the critical injection luminosities are of the same order, but correspond to slightly higher photon energies. Finally, in the case

of SMBHs with $\mathcal{M}_8 < 1$ (e.g., Seyfert galaxies), the critical luminosities at $\sim (1-10)\,\mathrm{GeV}$ photon energies can be as low as $\sim (10^{38}-10^{39})\,\mathrm{erg\ s^{-1}}$.

The application discussed above may be however complicated by the fact that in active nuclei γ-rays possibly produced in the immediate vicinities of SMBHs may be in addition absorbed by the 'external' low-energy radiation of the accreting matter. In order to estimate such an additional opacity, we write $\tau_{\rm ext} = (1/3)\,\sigma_{\rm T}\,R\,U_{\rm ext}/\varepsilon_{\rm ext}$, where $U_{\rm ext}$ is the monochromatic energy density of the accretion-related emission at photon energies $\varepsilon_{\rm ext} = 2\,m_{\rm e}^2 c^4/\varepsilon^\star$ within the volume R. This energy density can be found as $U_{\rm ext} = \zeta\,L_{\rm acc}/(4\pi\,R^2\,c)$, where we take conservatively $\zeta \approx 0.1$ since for $\varepsilon^\star$ corresponding to $B \approx (10^{-1}-10^4)\,\mathrm{G}$ the low-energy photons $\varepsilon_{\rm ext} \sim (10-300)\,\mathrm{eV}$ are of interest. Thus, with Eq. (1) and the assumed scaling Eq. (11) one obtains

$$\tau_{\rm ext} \approx 200\left(\frac{R}{\rm pc}\right)\left(\frac{B}{\rm G}\right)^{5/3} \quad . \tag{12}$$

For the considered parameter range, $\tau_{\rm ext}$ values are plotted in Figure 2 as light gray area in between of the thin solid ($R = 10^{-3}\,\mathrm{pc}$) and dashed ($R = 10^{-7}\,\mathrm{pc}$) lines (see the right y-axis). As shown, automatic quenching of high-energy γ-ray emission generated in the immediate vicinities of SMBHs can compete with the opacity due to emission of the accreting matter only in the case of very low accretion rates or low black hole masses.

5. Conclusions

The resonance-like behavior of the photon-photon annihilation cross section means that, for a wide range of magnetic field intensities between $B = 10^{-9}\,\mathrm{G}$ and $10^6\,\mathrm{G}$, γ-ray photons with energies between $\varepsilon \approx 0.3\,\mathrm{GeV}$ and $30\,\mathrm{TeV}$ (see Eq. 1) can be absorbed on the synchrotron radiation of pairs created in the annihilation process. This photon energy range is now, or will in the near future, be accessible to the *AGILE* and *GLAST* satellites, together with the ground based Imaging Atmospheric Cherenkov Telescopes *HESS*, *MAGIC*, *CANGAROO*, and *VERITAS*. The nonlinear dynamics of these γ-ray sources render them unstable to runaway pair production provided $\ell_{\rm inj} > 3$, where $\ell_{\rm inj} \equiv \varepsilon\,L_{\rm inj}\sigma_{\rm T}/(4\pi\,m_{\rm e}^2 c^5\,R)$ is the injection compactness of the source with the intrinsic monochromatic luminosity $L_{\rm inj}$ at photon energies ε, and with the spatial scale R. The spontaneously produced optical depth to absorption saturates at value greater than unity for photons with energies above ε, if $\ell_{\rm inj} \geq 6 + 36/(\eta\,\ell_{\rm B})$, where $\eta \approx 5^{1.5}$ and $\ell_{\rm B} \equiv \varepsilon\,U_{\rm B}\,R\,\sigma_{\rm T}/(m_{\rm e}^2\,c^4)$ is the magnetic compactness corresponding to the magnetic field energy density $U_{\rm B} = B^2/8\pi$. In this case the source automatically quenches its own γ-ray emission. As a corollary, we find that systems with small $\ell_{\rm B} < 1$ but large $\ell_{\rm inj} > 3$ suffer significant pair loading by this process. Gamma-ray

sources in the vicinity of active, supermassive black holes can be automatically quenched and the jets of these objects can by loaded with electron-positron pairs even at very low accretion rates or for low black hole masses.

Ł.S. was supported by MEiN through the research project 1-P03D-003-29 in years 2005-2008.

REFERENCES

Akharonian, F. A., Kririllov-Ugriumov, V. G., & Vardanian, V. V. 1985, Ap&SS, 115, 201

Boldt, E., & Ghosh, P. 1999, MNRAS, 307, 491

Boldt, E., & Loewenstein, M. 2000, MNRAS, 316, L29

Bonometto, S., & Rees, M. J. 1971, MNRAS, 152, 21

Coppi, P. S. 1992, MNRAS, 258, 657

Coppi, P. S., & Blandford, R. D. 1990, MNRAS, 245, 453

Fabian, A. C., Guilbert, P. W., Blandford, R. D., Phinney, E. S., & Cuellar, L. 1986, MNRAS, 221, 931

Gradshteyn, I. S., & Ryzhik, I. M. 1980, Table of integrals, series, and products (Academic Press inc., New York, New York)

Guilbert, P. W., Fabian, A. C., & Rees, M. J. 1983, MNRAS, 205, 593

Herterich, K. 1974, Nature, 250, 311

Jelley, J. V. 1966, Nature, 211, 472

Kazanas, D. 1984, ApJ, 287, 112

Kazanas, D., Georganopoulos, M., & Mastichiadis, A. 2002, ApJ, 578, L15

Kazanas, D., & Mastichiadis, A. 1999, ApJ, 518, L17

Kirk, J. G., & Mastichiadis, A. 1992, Nature, 360, 135

Konopelko, A. K., Kirk, J. G., Stecker, F. W., & Mastichiadis, A. 1999, ApJ, 518, L13

Krawczynski, H., Coppi, P. S., & Aharonian, F. 2002, MNRAS, 336, 721

Levinson, A. 2000, Physical Review Letters, 85, 912

Lightman, A. P., & Zdziarski, A. A. 1987, ApJ, 319, 643

Mastichiadis, A., & Kazanas, D. 2006, ApJ, 645, 416

Mastichiadis, A., & Kirk, J. G. 1995, A&A, 295, 613

Moderski, R., Sikora, M., Coppi, P. S., & Aharonian, F. 2005, MNRAS, 363, 954

Protheroe, R. J. 1986, MNRAS, 221, 769

Stern, B. E. 2003, MNRAS, 345, 590

Stern, B. E., Begelman, M. C., Sikora, M., & Svensson, R. 1995, MNRAS, 272, 291

Stern, B. E., & Poutanen, J. 2006, MNRAS, 372, 1217

Svensson, R. 1987, MNRAS, 227, 403

Zdziarski, A. A. 1988, ApJ, 335, 786

Zdziarski, A. A., & Lightman, A. P. 1985, ApJ, 294, L79

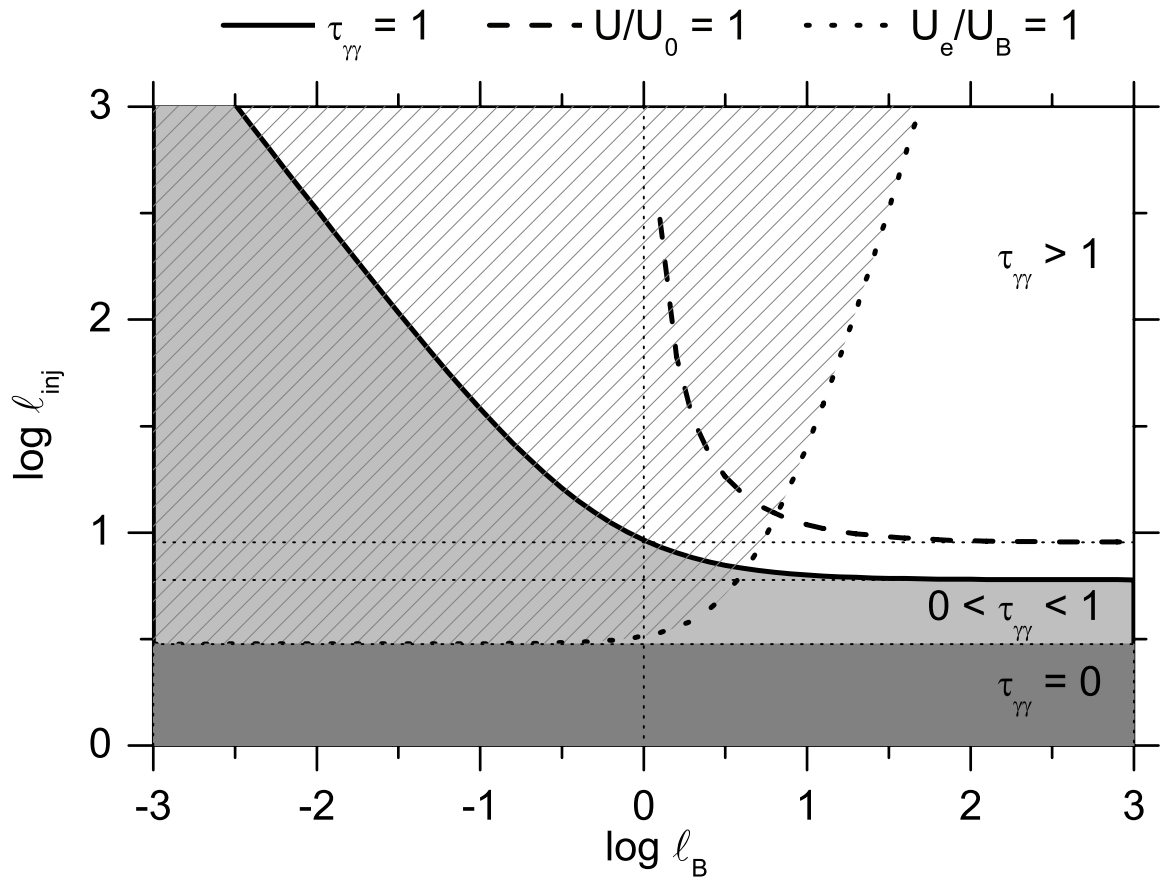

Fig. 1.— Properties of the stable solutions to the dynamical system 7. The dark gray shading denotes solutions with no electrons or soft photons, light gray shading denotes solutions with optical depth to photon-photon absorption less than unity and in the white area strong absorption occurs. The hatched area denotes solutions in which the energy density of the created pairs exceeds that in the magnetic field. The dashed line is the locus of points at which the energy density in soft photons formally reaches equipartition with that in hard photons.

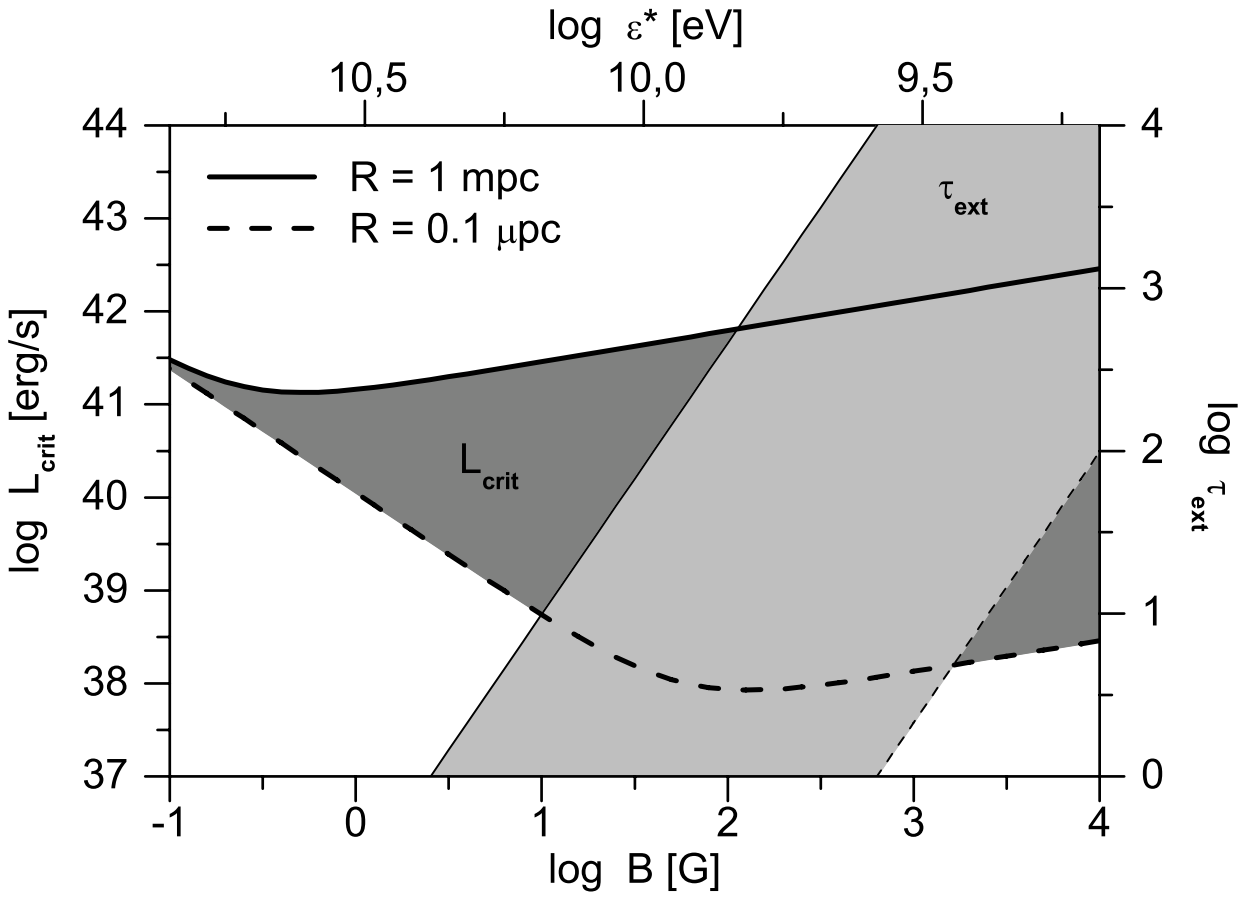

Fig. 2.— The critical injection luminosity $L_{\rm crit}$ that automatically generates a pair density and soft photon field of unit optical depth to photon-photon absorption, as a function of the magnetic field B and the pair energy $\varepsilon^\star$ (dark gray area between thick solid and dashed lines; left y-axis). For comparison, the expected opacity for the $\varepsilon^\star$ photons due to the emission of accreting matter is plotted (light gray area between thin solid and dashed lines; right y-axis).